A Study of Solid $[\{Cu(MePY2)\}_2O_2]^{2+}$ Using Resonance Raman and X-ray Absorption Spectroscopies: An Intermediate Cu_2O_2 Core Structure or a Solid Solution?

Elna Pidcock,[†] Serena DeBeer,[†] Honorio V. Obias,[‡] Britt Hedman,*[,†,§] Keith O. Hodgson,*[,†,§] Kenneth D. Karlin,*[,‡] and Edward I. Solomon*[,†]

Contribution from the Department of Chemistry, Stanford University and Stanford Synchrotron Radiation Laboratory, SLAC, Stanford, California 94305, and Department of Chemistry, Johns Hopkins University, Baltimore, Maryland 21218

Received September 28, 1998

Abstract: Solid $[\{Cu(MePY2)\}_2O_2]^{2+}$ is spectroscopically characterized using resonance Raman and X-ray absorption spectroscopy, for which the former technique probes the nature of the O−O bond and the latter defines the Cu−Cu interaction. In contrast to the crystal structure obtained for $[\{Cu(MePY2)\}_2O_2]^{2+}$, which shows an "intermediate" Cu_2O_2 core (Cu−Cu = 3.4 Å and O−O = 1.6 Å), resonance Raman peaks characteristic of both a side-on peroxide-bridged dicopper(II) core and bis-μ-oxo dicopper(III) core are observed. The bis-μ-oxo isomer is estimated to be present at approximately 5−20%. A good fit is obtained for EXAFS data for solid $[\{Cu(MePY2)\}_2O_2]^{2+}$ using an 80:20 ratio of Cu−Cu separations of 3.6 Å (characteristic of a side-on peroxide-bridged copper core) and 2.8 Å (associated with a bis-μ-oxo dicopper core). Analysis of the edge region places an upper limit on the amount of bis-μ-oxo isomer present in the solid at 40%. The factors governing the presence of bis-μ-oxo and/or side-on peroxide cores in solution for differing ligand systems are considered, and the contribution of the bite angle of the equatorial nitrogen atom donors is explored. The reactivity of $[\{Cu(MePY2)\}_2O_2]^{2+}$ in solution is correlated with the presence of the bis-μ-oxo core, using frontier molecular orbital theory.

Introduction

The oxygen transport protein hemocyanin and the monooxygenase enzyme tyrosinase have been studied extensively.[1,2] A crystal structure obtained of the oxy form of hemocyanin (oxyHc) showed oxygen bound as peroxide in a side-on, μ-η^2:η^2 fashion between the two copper(II) centers.[3] The electronic absorption spectrum of oxyHc has bands at 345 nm (ϵ = 20 000 M^{-1} cm^{-1}) and a weak band at 570 nm (ϵ = 1000 M^{-1} cm^{-1}), and the peroxide O−O stretch is observed at 740 cm^{-1}.[4] The absorption and resonance Raman spectra collected for oxy-tyrosinase are very similar to those obtained for oxyhemocyanin, and it is generally accepted that tyrosinase also binds peroxide in a $[Cu_2(\mu\text{-}\eta^2\text{:}\eta^2)(O_2)]^{2+}$ core. Tyrosinase activates O_2 for reaction with phenols, oxygenating them to *o*-quinones.[5] It has been shown that the monophenol substrate binds directly to copper at the active site,[6] but it has not been established whether O−O bond scission occurs prior to, or concomitant with, substrate activation. This question has become increasingly important with the isolation of $[Cu(III)_2(\mu\text{-}O)_2]^{2+}$ cores, (characterized by intense absorption bands at 300−350 nm and 400−450 nm and an intense resonance Raman peak assigned as a Cu−O stretch at ∼600 cm^{-1}),[7,8] and the demonstration that interconversion of the $[Cu_2(\mu\text{-}\eta^2\text{:}\eta^2)(O_2)]^{2+}$ and $[Cu(III)_2(\mu\text{-}O)_2]^{2+}$ cores can be effected by changing the solvent.[9]

Studies performed on a series of complexes, $[Cu_2(N\mathit{n}PY2)(O_2)]^{2+}$ (where two bis(2-pyridylethyl) amine units (PY2) are linked via the amino nitrogen by a $-(CH_2)_n-$ chain (where n = 3,4,5)) showed that dioxygen is bound in a side-on, μ-η^2:η^2 fashion.[10] The absorption spectra of the peroxide-bridged binuclear copper cores have bands characteristic of a planar side-on peroxide core at 360 nm and 520−600 nm (depending on the length of the alkyl chain) as well as an additional band in the region 420−490 nm.[11,12] It was established that the "extra"

* To whom correspondence should be addressed at Stanford University. Prof. E. I. Solomon: FAX: (650) 725-0259. E-mail: solomon@chem.stanford.edu.

[†]Department of Chemistry, Stanford University.

[‡]Department of Chemistry, Johns Hopkins University.

[§] Stanford Synchrotron Radiation Laboratory, SLAC, Stanford University.

(1) (a) Eickman, N. C.; Himmelwright, R. S.; Solomon, E. I. *Proc. Natl. Acad. Sci. U.S.A.* **1979**, *76*, 2094−2098. (b) Lowery, M. D.; Solomon, E. I. *Science* **1993**, *259*, 1575−1581. (c) Solomon, E. I.; Sundaram, U. M.; Machonkin, T. E. *Chem. Rev.* **1996**, *96*, 2563−2605. (d) Magnus, K. A.; Ton-That, H.; Carpenter, J. E. *Chem. Rev.* **1994**, *94*, 727−735.

(2) (a) Lerch, K. *Enzymatic Browning and its Prevention*; American Chemical Society: Washington, DC, 1995. (b) Sánchez-Ferrer, A.; Rodríguez-López, J. N.; García-Cánovas, F.; García-Carmona, F. *Biochim. Biophys. Acta* **1995**, *1247*, 1−11.

(3) Magnus, K. A.; Hazes, B.; Ton-That, H.; Bonaventura, C.; Bonaventura, J.; Hol, W. J. G. *Proteins* **1994**, *19*, 302−309.

(4) Solomon, E. I.; Baldwin, M. J.; Lowery, M. D. *Chem. Rev.* **1992**, *92*, 521−542.

(5) Jolley, R. L.; Evans, L. H.; Makino, N.; Mason, H. S. *J. Biol. Chem.* **1974**, *249*, 335−345.

(6) Wilcox, D. E.; Porras, A. G.; Hwang, Y. T.; Lerch, K.; Winkler, M. E.; Solomon, E. I. *J. Am. Chem. Soc.* **1985**, *107*, 4015−4027.

(7) Mahapatra, S.; Halfen, J. A.; Wilkinson, E. C.; Pan, G.; Wang, X.; Young, V. G.; Cramer, C. J.; Que, L., Jr.; Tolman, W. B. *J. Am. Chem. Soc.* **1996**, *118*, 11555−11574.

(8) Mahadevan, V.; Hou, Z. G.; Cole, A. P.; Root, D. E.; Lal, T. K.; Solomon, E. I.; Stack, T. D. P. *J. Am. Chem. Soc.* **1997**, *119*, 11996−11997.

(9) Halfen, J. A.; Mahapatra, S.; Wilkinson, E. C.; Kaderli, S.; Young, V. G.; Que, L., Jr.; Zuberbühler, A. D.; Tolman, W. B. *Science* **1996**, *271*, 1397−1400.

(10) Pidcock, E.; Obias, H. V.; Abe, M.; Liang, H.-C.; Karlin, K. D.; Solomon, E. I. *J. Am. Chem. Soc.* **1999**, *121*, 1299−1308.

10.1021/ja983444s CCC: $18.00
Published on Web 02/20/1999

Scheme 1

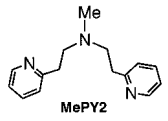

band is an $O_2^{2-} \rightarrow$ Cu(II) CT band, and its energy and intensity are correlated with the degree of "butterflying" of the Cu_2O_2 plane due to the short methylene linker.[10] The more planar the core, the higher the energy and the lower the intensity of the $O_2^{2-} \rightarrow$ Cu(II) CT band at 420−490 nm. In the planar limit, e.g., [Cu(HB(3,5-*i*-Pr$_2$pz)$_3$)]$_2$(O$_2$),[13] this band has no intensity.

A related series of complexes, $[Cu_2(XYL)]^{2+}$, where the Cu(PY2) centers are linked, not by an alkyl chain but by a xylyl unit, react with dioxygen and hydroxylate the arene ring of the ligand.[14,15] The absorption spectrum of the O_2 bound intermediate in $[Cu_2(NO_2\text{-}XYL)(O_2)]^{2+}$ is very similar to those obtained for the $[Cu_2(N\mathit{n}PY2)(O_2)]^{2+}$ series, with bands at 358 nm (ϵ = 20 000 M^{-1} cm^{-1}), 435 nm (ϵ = 5000 M^{-1} cm^{-1}), and 530 nm (ϵ = 1200 M^{-1} cm^{-1}).[14] It was determined, using resonance Raman spectroscopy, that dioxygen binds as peroxide in a side-on geometry and that it is this species and not an unobservable amount of bis-μ-oxo isomer which is likely to be the reactive intermediate in the electrophilic attack of the aromatic ring in the hydroxylation reaction.[16]

A mononuclear complex $[Cu(I)(MePY2)]^+$, (Scheme 1) where the amine nitrogen of the PY2 unit is substituted with a methyl group (cf. the N*n* series where the PY2 units are linked by an alkyl chain) reacts with dioxygen to form a binuclear complex $[\{Cu(MePY2)\}_2O_2]^{2+}$ with an absorption spectrum similar to those observed for both $[Cu_2(N\mathit{n}PY2)(O_2)]^{2+}$ and $[Cu_2(NO_2\text{-}XYL)(O_2)]^{2+}$, with bands at 355 nm ($\epsilon$ (M^{-1} cm^{-1}) 14 700), 410 nm (2500) and 530 nm (400).[17]

The geometry at the two copper centers of the binuclear $[\{Cu(MePY2)\}_2O_2]^{2+}$ complex is unconstrained by the presence of a linker, and hence the Cu_2O_2 unit is expected to be close to planar; the additional band observed in the absorption spectra obtained for the linked Cu(PY2)-containing complexes should have no intensity in the planar Cu_2O_2 core (vide supra). Resonance Raman spectroscopic studies for solutions of $[\{Cu(MePY2)\}_2O_2]^{2+}$ have shown that the extra band at 410 nm is not due to a butterfly Cu_2O_2 core, but rather to the presence of a small amount (1−10%) of the bis-μ-oxo isomer, in contrast to the results obtained for $[Cu_2(N\mathit{n}PY2)(O_2)]^{2+}$ and $[Cu_2(NO_2\text{-}XYL)(O_2)]^{2+}$.[18] It has been observed that $[\{Cu(MePY2)\}_2O_2]^{2+}$ in solution can effect clean H-atom abstraction reactions with exogenously added hydrocarbon substrates, reactivity which is *not* observed for binuclear copper complexes with linked PY2 units, $[Cu_2(N\mathit{n}PY2)(O_2)]^{2+}$ and $[Cu_2(NO_2\text{-}XYL)(O_2)]^{2+}$.

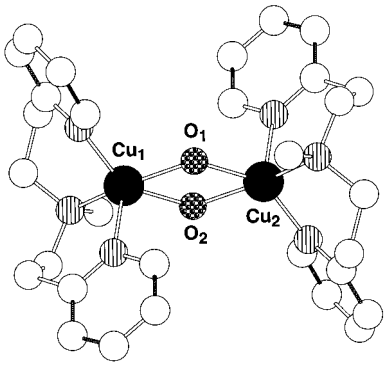

Figure 1. X-ray crystal structure of $[\{Cu(MePY2)\}_2O_2](BArF)_2$. The bond distances and angles for the Cu_2O_2 core are as follows: Cu_1-Cu_2 = 3.445(2) Å, Cu_1-O_1 = 1.905(5) Å, O_1-Cu_2 = 1.922(6) Å, O_1-O_2 = 1.666(12) Å, $O_1-Cu_1-O_2$ = 51.6(3)°, $Cu_1-O_1-Cu_2$ = 128.4(3)°.

An X-ray crystal structure has been obtained for $[\{Cu(MePY2)\}_2(O_2)]^{2+}$.[19,20] Surprisingly, the copper−copper separation was found to be 3.45 Å, and the O−O distance was 1.67 Å (Figure 1); a structure which is intermediate between that of a side-on peroxide core (Cu−Cu = 3.6 and O−O = 1.41 Å) and a bis-μ-oxo core (Cu···Cu = 2.9 and O−O = 2.3 Å).

We have studied the solid form of $[\{Cu(MePY2)\}_2O_2]^{2+}$ using resonance Raman spectroscopy to probe the nature of the bound dioxygen and X-ray absorption spectroscopy (XAS) to examine the copper−copper interaction to establish whether solid $[\{Cu(MePY2)\}_2O_2]^{2+}$ comprises a mixture of the side-on peroxide and bis-μ-oxo isomers, analogous to the solution, or if the "intermediate" core dimensions given by the crystal structure represent the true structure. A discussion of the reactivity observed for $[\{Cu(MePY2)\}_2O_2]^{2+}$ in solution and the factors which govern the formation of side-on peroxide and bis-μ-oxo isomers is presented.

Experimental Section

Preparation of [{Cu(MePY2)}$_2$(O$_2$)]$^{2+}$. Under a blanket of argon, 1 mmol of [(MePY2)Cu(I)(CH$_3$CN)][BArF][18] (where BArF is B[3,5-(CF$_3$)$_2$C$_6$H$_3$]$_4^-$) and a spin bar were transferred to a 100-mL flame-dried Schlenk flask. Then, 40 mL of freshly distilled, degassed dichloromethane was added. The yellow solution was stirred for 15 min and filtered through a medium-sized frit into another flame-dried 100-mL Schlenk flask. This solution was cooled to −95 °C (methanol/liquid nitrogen bath) and stirred at this temperature for 15 min. The cold, yellow solution was bubbled through with ultrahigh purity dioxygen (99.999%), passed through two cold traps maintained at −78 and −10 °C for about 1−5 min. Formation of a dark colored solution was observed. The solution was allowed to stand at this temperature for 30 min, whereupon 80 mL of precooled (−10 °C) freshly distilled degassed heptane was added dropwise. The resulting mixture was kept at this temperature for a few hours until the supernatant was almost clear. The brown precipitate was filtered through a precooled coarse frit maintained at −100 °C. Precooled heptane was used to wash the precipitate, followed by precooled pentane.

Resonance Raman Spectroscopy. Resonance Raman data were obtained using a Princeton Instruments ST-135 back-

(11) Karlin, K. D.; Tyeklár, Z.; Farooq, A.; Haka, M. S.; Ghosh, P.; Cruse, R. W.; Gultneh, Y.; Hayes, J. C.; Zubieta, J. *Inorg. Chem.* **1992**, *31*, 1436−1451.
(12) Karlin, K. D.; Haka, M. S.; Cruse, R. W.; Meyer, G. J.; Farooq, A.; Gultneh, Y.; Hayes, J. C.; Zubieta, J. *J. Am. Chem. Soc.* **1988**, *110*, 1196−1207.
(13) Kitajima, N.; Fujisawa, K.; Fujimoto, C.; Moro-oka, Y.; Hashimoto, S.; Kitagawa, T.; Toriumi, K.; Tatsumi, K.; Nakamura, A. *J. Am. Chem. Soc.* **1992**, *114*, 1277−1291.
(14) Karlin, K. D.; Nasir, M. S.; Cohen, B. I.; Cruse, R. W.; Kaderli, S.; Zuberbühler, A. D. *J. Am. Chem. Soc.* **1994**, *116*, 1324−1336.
(15) Karlin, K. D.; Hayes, J. C.; Gultneh, Y.; Cruse, R. W.; McKown, J. W.; Hutchinson, J. P.; Zubieta, J. *J. Am. Chem. Soc.* **1984**, *106*, 2121−2128.
(16) Pidcock, E.; Obias, H. V.; Xin Zhang, C.; Karlin, K. D.; Solomon, E. I. *J. Am. Chem. Soc.* **1998**, *120*, 7841−7847.
(17) Sanyal, I.; Mahroof-Tahir, M.; Nasir, M. S.; Ghosh, P.; Cohen, B. I.; Gultneh, Y.; Cruse, R. W.; Farooq, A.; Karlin, K. D.; Lui, S.; Zubieta, J. *Inorg. Chem.* **1992**, *31*, 4322−4332.
(18) Obias, H. V.; Lin, Y.; Murthy, N. N.; Pidcock, E.; Solomon, E. I.; Ralle, M.; Blackburn, N. J.; Neuhold, Y.-M.; Zuberbühler, A. D.; Karlin, K. D. *J. Am. Chem. Soc.* **1998**, *120*, 12960−12961.
(19) H. V. Obias, 1998, Ph.D. Dissertation, Johns Hopkins University
(20) Obias, H. V.; Lin, Y.; Murthy, N. N.; Neuhold, Y.-M.; Zuberbühler, A. D.; Karlin, K. D., manuscript in preparation.

illuminated CCD detector on a Spex 1877 CP triple monochromator with 1200, 1800, and 2400 grooves/mm holographic spectrograph gratings. The excitation was provided by Coherent I90C-K Kr+ and Innova Sabre 25/7 Ar+ CW lasers. A polarization scrambler was used between the sample and the spectrometer. Spectral resolution was <2 cm^{-1}. Samples for solid Raman spectra were prepared by removing crystalline solid from dichloromethane/heptane mother liquor and drying the solid on filter paper before grinding the material to a fine powder. The powdered solid was placed in a NMR tube. All procedures were performed over dry ice at −78 °C. The sample tube was spun with an air-driven NMR spinner and cooled to ∼180 K by an N_2-flow system.

XAS Data Collection and Reduction. XAS samples of [{Cu(MePY2)}$_2$(O$_2$)](BArF)$_2$ were prepared as solids in boron nitride. The mixture was ground over dry ice, pressed into a pellet, and sealed between 63.5-μm Mylar tape windows in a 1-mm aluminum spacer. The sample was immediately frozen by immersion in liquid nitrogen and maintained at this temperature or lower throughout.

XAS data were collected at the Stanford Synchrotron Radiation Laboratory (SSRL) on unfocused 8-pole wiggler beamline 7−3 under ring conditions 3.0 GeV and 60−100 mA. A Si(220) monochromator was utilized for energy selection at the Cu K-edge. The monochromator was detuned 50% to minimize higher harmonic components in the X-ray beam. The samples were maintained at 10 K during the data collection using an Oxford Instruments CF1208 continuous flow liquid helium cryostat. Data were measured in transmission mode to $k = 13.4$ Å^{-1} (the zinc K-edge), as it was found that the model complex contained small quantities of zinc. Internal energy calibration was performed by simultaneous measurement of the absorption of a Cu foil placed between a second and third ionization chamber. The first inflection point was assigned to 8980.3 eV. The data represent a 2-scan average.

Data were processed as described previously,[21] by fitting a second-order polynomial to the postedge region and subtracting this background from the entire spectrum. A three-region cubic spline was used to model the smooth background above the edge. Normalization of the data was achieved by subtracting the spline and normalizing the edge jump to 1.0 at 9000 eV. Theoretical EXAFS signals $\chi(k)$ were calculated using *FEFF* (version 6.0)[22,23] and fit to the data using EXAFSPAK (G. N. George, SSRL). The structural parameters varied during the refinements were the bond distance (R) and the bond variance (σ^2). The σ^2 is related to the Debye−Waller factor, which is a measure of thermal vibration and static disorder of the absorbers/scatterers. In addition the nonstructural parameter, E_o, which defines the origin of the photoelectron wave vector (k), was allowed to vary in order to align the ionization threshold of the theoretical signal to that of the experimental data. Coordination numbers were systematically varied in the course of the analysis but were not allowed to vary within a given fit. Single scattering paths and the corresponding multiple scattering paths were linked during intial refinements and were allowed to float independently in the final fits.

Density Functional Calculations. LCAO density functional calculations were performed using the 2.0.1 version of the Amsterdam Density Functional (ADF) programs.[24] The Vosko−Wilk−Nusair local density approximation[25] for the exchange and correlation energy was used with nonlocal gradient corrections of Becke[26] and Perdew.[27] A triple-ζ Slater-type orbital (STO) basis set with a single-ζ STO polarization function was used for all atoms. Filled-shell orbitals were treated by the frozen core approximation.

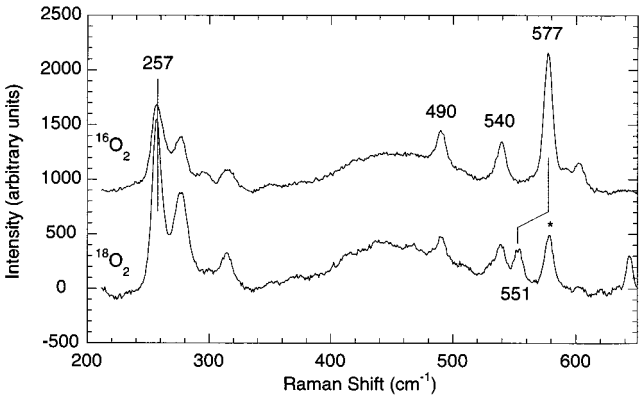

Figure 2. Resonance Raman spectra obtained with $^{16}O_2$ (top) and $^{18}O_2$ (bottom) of solid [{Cu(MePY2)}$_2$O$_2$]$^{2+}$, with an excitation wavelength of 406.9 nm. The peak labeled with an asterisk in the $^{18}O_2$ spectrum is derived from $^{16}O_2$ contamination.

Results and Analysis

Resonance Raman Spectroscopy. Resonance Raman spectra of solid [{Cu(MePY2)}$_2$(^{16}O$_2$)]$^{2+}$ and [{Cu(MePY2)}$_2$(^{18}O$_2$)]$^{2+}$ were obtained with an excitation wavelength of 406.9 nm (Figure 2), nearly coincident with the shoulder observed in the absorption spectrum.[18] An intense Raman peak is observed at 577 cm^{-1} which shifts upon $^{18}O_2$ substitution to 551 cm^{-1}. A Raman peak at 257 cm^{-1} is also observed which does not shift with isotopic substitution of the oxygen atoms. Resonance Raman spectra of [{Cu(MePY2)}$_2$O$_2$]$^{2+}$ were obtained at two additional wavelengths, 363.9 nm, nearly coincident with the highest-energy, intense LMCT absorption band at 355 nm, and 386 nm. The relative intensities of the Raman peaks at 577 and 257 cm^{-1} change with excitation wavelength; the ratio of the intensity of the peak at 577 cm^{-1} to the intensity of the peak at 257 cm^{-1} is greatest at an excitation wavelength of 406.9 nm and smallest at an excitation wavelength of 363.9 nm (Figure 3).

In analogy to the vibrational data obtained for the side-on peroxide dicopper core in [Cu(HB(3,5-Ph$_2$pz)$_3$)]$_2$O$_2$,[28] the Raman peak at 257 cm^{-1} is assigned to the symmetric Cu$_2$(O$_2$) stretch which primarily involves copper motion (Cu−Cu stretch), and hence shows no $^{18}O_2$ isotope dependence. The increase in intensity of this Raman peak, as the excitation wavelength approaches λ_{max} of the highest-energy LMCT transition is also consistent with its assignment as the low-energy Cu−Cu stretch of a side-on peroxide core; resonance Raman profiles of the Cu−Cu stretch at 297 cm^{-1} in [Cu(HB(3,5-Ph$_2$pz)$_3$)]$_2$O$_2$ showed strong enhancement from the peroxide to Cu(II) CT at 360 nm.[28]

The Raman peak at 577 cm^{-1} in [{Cu(MePY2)}$_2$O$_2$]$^{2+}$ shows a shift of 26 cm^{-1} upon substitution with $^{18}O_2$. The O−O stretch

(21) DeWitt, J. G.; Bentsen, J. G.; Rosenzweig, A. C.; Hedman, B.; Green, J.; Pilkington, S.; Papaefthymiou, G. C.; Dalton, H.; Hodgson, K. O.; Lippard, S. J. *J. Am. Chem. Soc.* **1991**, *113*, 9219−9235.
(22) Rehr, J. J.; Mustre de Leon, J.; Zabinsky, S. I.; Albers, R. C. *J. Am. Chem. Soc.* **1991**, *113*, 5135−5140.
(23) Mustre de Leon, J.; Rehr, J. J.; Zabinsky, S. I.; Albers, R. C. *Phys. Rev.* **1991**, *B44*, 4146−4156.
(24) te Velde, G.; Baerends, E. J. *J. Comput. Phys.* **1992**, *99*, 84−98.
(25) Vosko, S. H.; Wilk, L.; Nusair, M. *Can. J. Phys.* **1980**, *58*, 1200−1211.
(26) Becke, A. D. *Phys. Rev. A* **1988**, *38*, 3098−3100.
(27) Perdew, J. P. *Phys. Rev. B* **1986**, *33*, 8800−8802.
(28) Baldwin, M. J.; Root, D. E.; Pate, J. E.; Fujisawa, K.; Kitajima, N.; Solomon, E. I. *J. Am. Chem. Soc.* **1992**, *114*, 10421−10431.

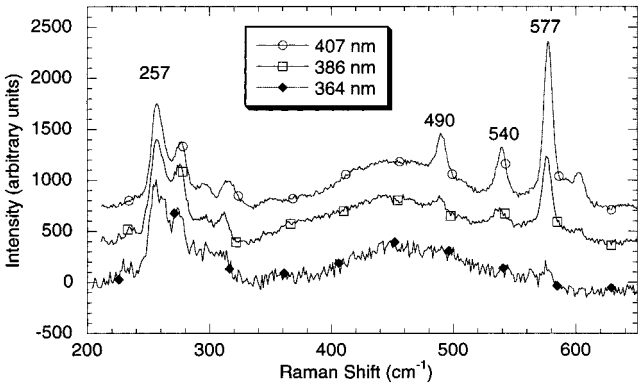

Figure 3. Resonance Raman spectra obtained of solid [{Cu(MePY2)}$_2$O$_2$]$^{2+}$ using excitation wavelengths of 406.9, 386, and 364 nm. Intensities of the Cu−Cu stretches at 257 cm^{-1} are normalized to an arbitrary value of 1000.

of the side-on peroxide core in oxyHc (O−O = 1.4 Å) is observed at 740 cm^{-1} and shifts ~40 cm^{-1} upon isotopic substitution.[4] The low frequency and small isotope shift of the Raman band at 577 cm^{-1} in [{Cu(MePY2)}$_2$O$_2$]$^{2+}$ eliminates its assignment as an O−O stretch of this side-on peroxide core. To evaluate the intermediate structure indicated by crystallography, the force constant for an O−O bond length of 1.67 Å was estimated using Badger's Rule, which correlates force constant and bond length.[29] The calculated frequency of such a stretch is 522 cm^{-1}, and the isotope shift calculated assuming a simple harmonic oscillator is 30 cm^{-1}. Therefore, the intense stretch observed at 577 cm^{-1} cannot be assigned as an O−O stretch associated with the Cu$_2$O$_2$ core with O−O = 1.67 Å, indicated by the crystal structure. However, the observed isotope shift of the stretch at 577 cm^{-1} (Δ = 26 cm^{-1}) is in excellent agreement with the expected shift of 26 cm^{-1} for a simple Cu$_2$(O)$_2$ harmonic oscillator at 577 cm^{-1} and therefore the peak at 577 cm^{-1} is assigned as a Cu−O stretch. One possibility is that the intense stretch at 577 cm^{-1} is an asymmetric Cu−O vibration associated with the side-on peroxide core. If this were the case, the profile of the stretch would be expected to be similar to that of the low energy Cu−Cu stretch at 257 cm^{-1}. However, the peak at 577 cm^{-1} is most intense when an excitation wavelength of 406.9 nm (nearly coincident with the shoulder in the absorption spectrum at 410 nm) is used: the excitation wavelength at which the Cu−Cu stretch at 257 cm^{-1} is the weakest. The intensity of the stretch at 577 cm^{-1} is high; this is also not consistent with its possible assignment as a formally forbidden, asymmetric stretch.

The absorption spectra of the [Cu(III)$_2$(μ-O)$_2$]$^{2+}$ cores[7−9] have absorption bands in the 400−450 nm region; resonance Raman spectra obtained using excitation wavelengths coincident with these bands show a characteristic, intense Cu−O stretch at ~600 cm^{-1} which shifts 20−25 cm^{-1} upon ^{18}O$_2$ substitution. Therefore, the intense stretch observed at 577 cm^{-1} observed in [{Cu(MePY2)}$_2$O$_2$]$^{2+}$ is assigned as the symmetric Cu−O core stretch of a [Cu(III)$_2$(μ-O)$_2$]$^{2+}$ core. The weak shoulder at 410 nm in the absorption spectrum of [{Cu(MePY2)}$_2$O$_2$]$^{2+}$ must be assigned as a μ-O^{2-} → Cu(III) CT transition. The Raman peaks seen at 490 and 540 cm^{-1}, which do not shift with ^{18}O$_2$ isotopic substitution and show profile behavior similar to that of the peak at 577 cm^{-1}, are comparable to bands observed for [Cu$_2$(TACN^{Bn3})$_2$(μ-O)$_2$]$^{2+}$ (where TACN^{R3} is an *N*,*N*′,*N*″-trisubstituted 1,4,7-triazacyclononane) and hence are also assigned as vibrations associated with the [Cu(III)$_2$(μ-O)$_2$]$^{2+}$ core.[7]

(29) Hershbach, D. E.; Laurie, V. W. *J. Chem. Phys.* **1961**, *35*, 458−463.

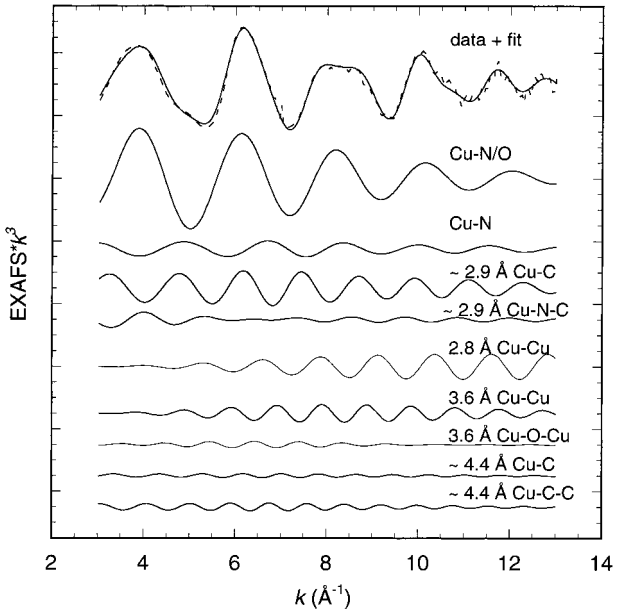

Figure 4. Individual EXAFS contributions and the total EXAFS signal (—), compared with the experimental data (- - -) for [{Cu(MePY2)}$_2$O$_2$]$^{2+}$. The fit represents an 80:20 mixture of 3.6 and 2.8 Å Cu−Cu contributions.

The results obtained from the resonance Raman study thus indicate that there is a mixture of side-on peroxide and bis-μ-oxo isomers present in solid [{Cu(MePY2)}$_2$(O$_2$)]$^{2+}$. By comparing the relative intensities of the stretches at 257 and 577 cm^{-1} obtained for the wavelengths 364, 386, and 407 nm with the intensities of the 287 cm^{-1} Cu−O stretch of [Cu$_2$(XYL-F)(μ-η^2:η^2)(O$_2$)]$^{2+}$ and the 609 cm^{-1} stretch of [(L$_{TM}$Cu)$_2$(μ-O)$_2$]$^{2+}$ [8] (where L$_{TM}$ is tetramethyl-cyclohexane diamine) in solutions of equal concentration for the same excitation wavelength range, it is estimated that the amount of bis-μ-oxo isomer present in solid [{Cu(MePY2)}$_2$O$_2$]$^{2+}$ is 5−20%.

Cu XAS. EXAFS. The k^3-weighted EXAFS data and the Fourier transform for [{Cu(MePY2)}$_2$O$_2$]$^{2+}$ are shown in Figures 4 (top) and 5, respectively. *FEFF* fits were initially performed using phase and amplitude parameters calculated from the crystallographic coordinates of [{Cu(MePY2)}$_2$O$_2$]$^{2+}$.[19,20] The fit results indicate poor agreement with the crystallographic results, particularly for the Cu$_2$O$_2$ core, showing no evidence for a Cu−Cu interaction at 3.45 Å. A Cu−Cu distance intermediate between that expected for a side-on peroxide core (3.6 Å) and a bis-μ-oxo core (2.9 Å) could not be obtained through least-squares refinements. To further evaluate this possibility, a fit in which the Cu−Cu distance was *fixed* at the crystallographic distance of 3.45 Å was attempted, allowing all other parameters to float. This fit (Figure 5a) shows a clear mismatch to the FT peak between 3 and 4 Å.

Since the Cu$_2$O$_2$ core parameters were found to differ significantly from the starting crystallographic model, the Cu−Cu and Cu−O bond distances were refined, and new amplitude and phase functions were calculated until no further changes were observed. An alternate model, using a side-on peroxide core and the same ligand set as MePY2, gave very reasonable fits to the data (Figure 5b). Curve-fitting results indicate that the first shell is well fit by 4 Cu−N/O interactions at 1.95 Å and 1 Cu−N interaction at 2.30 Å. The 4 Cu−N/O interactions have relatively high σ^2 values, indicating a relatively large distribution of scatterers. Attempts were made to separate this contribution into two components. This results in two separate components at 1.90 and 2.05 Å, which have more reasonable

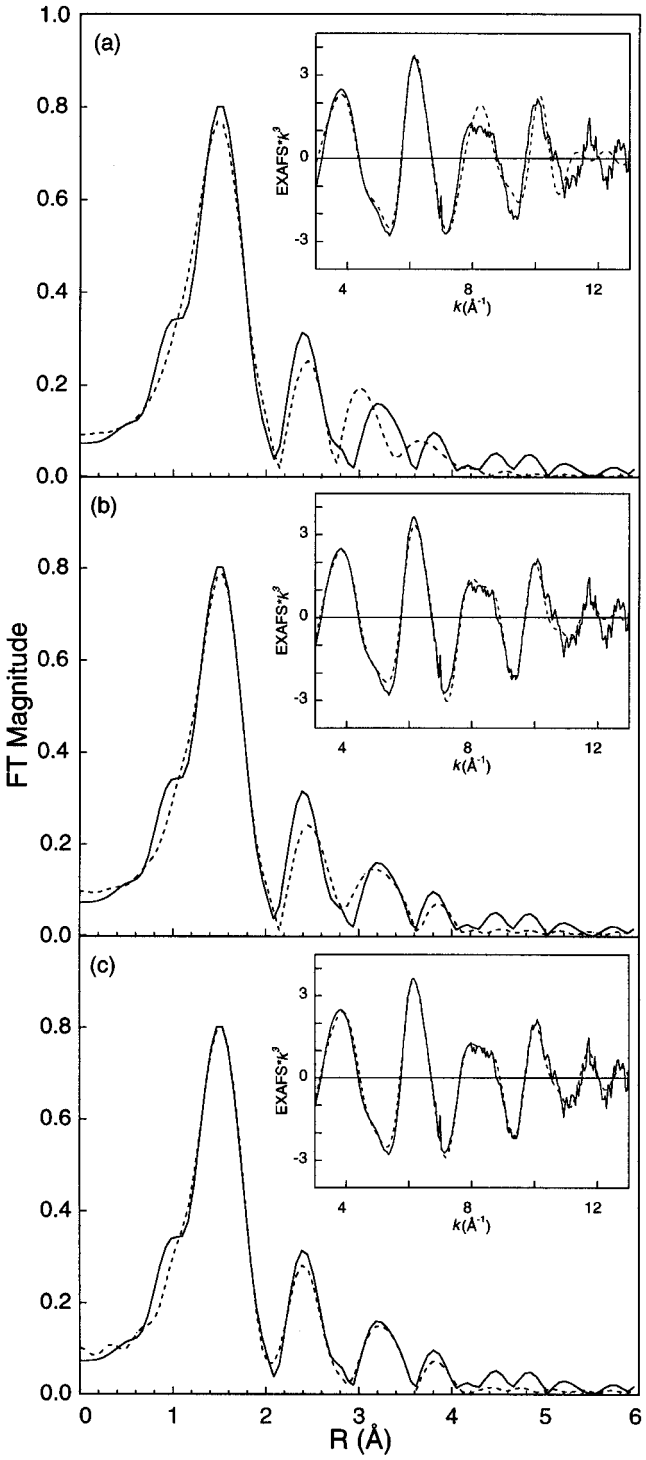

Figure 5. Non-phase shift-corrected Fourier transforms and EXAFS data (inset) for $[\{Cu(MePY2)\}_2O_2]^{2+}$ (—) and fits to the data (- - -) using (a) the crystallographic Cu−Cu distance of 3.45 Å, (b) 100% 3.6 Å Cu−Cu, and (c) a mixture of 80% 3.6 Å Cu−Cu and 20% 2.8 Å Cu−Cu.

σ^2 values. There is also an improvement in the fit function; however, separation of the two distances is not within the resolution of the data (since, $\Delta R = \pi/2\Delta k$). To fit the outer shells, inclusion of both single and multiple scattering interactions from the pyridine rings as well as a Cu−Cu single scattering and Cu−O−Cu multiple scattering interactions at 3.6 Å were necessary (Table 1).

Since the results of resonance Raman studies (vide supra) indicate a mixture of side-on peroxo and bis-μ-oxo core species is present, fits were attempted in which varying ratios of 3.6 and 2.8 Å Cu−Cu components were included. The results show that the data favor a side-on peroxo core structure, as a reasonable fit is obtained by inclusion of only a 3.6 Å Cu−Cu interaction and no 2.8 Å Cu−Cu component. An improvement to the fit is obtained by using an 80:20 mixture of 3.6 to 2.8 Å Cu−Cu (Figure 5c). However, this improvement may simply be attributed to the addition of two more free parameters. The fits obtained using 60:40, 40:60, and 20:80 mixtures of 3.6 Å to 2.8 Å Cu−Cu interactions produce visually similar results. It is only when no 3.6 Å Cu−Cu component is included, that a visually poor fit is obtained (not shown). This can be explained by examining two main trends in the fits. First, as the amount of 3.6 Å Cu−Cu is decreased the σ^2 value for this component decreases, hence this parameter compensates for the decrease in coordination number. When an unreasonably small amount of 3.6 Å Cu−Cu is present, i.e. when there is less than a 20% contribution, a physically unreasonably σ^2 value is obtained. When this component is not included, the outermost peak of the FT can no longer be fit. Second, as the fraction of 2.8 Å Cu−Cu increases, the σ^2 values for the Cu−C interactions at ∼2.9 Å decrease. As is seen in Figure 4, these two components are ∼180° out of phase. The fit results demonstrate that addition of a higher 2.8 Å Cu−Cu contribution is compensated for by strengthening of the σ^2 value for the 2.9 Å Cu−C interactions, followed by a subsequent shift in the Cu−C distances. Fits were also performed on filtered data, fitting only the FT peak between 2 and 3 Å. A similar trend is observed, showing that the Cu−Cu interaction is highly correlated to the Cu−C interactions at approximately the same distance. (Note, filtered data fits to the FT peak between 3 and 4 Å show that the 3.6 Å Cu−Cu component is not correlated to the Cu−C interactions at ∼4.3 Å).

In summary, the EXAFS results show no evidence for an intermediate structure. The presence of a 3.6 Å Cu−Cu distance in $[\{Cu(MePY2)\}_2O_2]^{2+}$ has been clearly established. Due to the correlation between the 2.8 Å Cu−Cu component and the Cu−C components at ∼2.9 Å, the amount of bis-μ-oxo cannot be determined from the EXAFS. However, the trend in *F* values suggests that the side-on peroxo species is favored.

Cu K-edge. The X-ray absorption edge of $[\{Cu(MePY2)\}_2O_2]^{2+}$ is shown in Figure 6. The edge is characteristic of Cu(II) and exhibits an essentially featureless pre-edge, with a maximum at ∼8979 eV, as shown in the second derivative. Conversely, the bis-μ-oxo species has been described as having Cu(III) sites, which exhibit a shift of ∼1.5−2.0 eV to higher energy in the pre-edge relative to analogous Cu(II) complexes.[30] To estimate the amount of bis-μ-oxo species present in $[\{Cu(MePY2)\}_2O_2]^{2+}$, simulated edges were calculated by adding spectra while proportionally varying the amount of known side-on peroxo and bis-μ-oxo models. Data of $([Cu(HB(3,5\text{-}Ph_2pz)_3]_2(O_2)$[13] and $[Cu_2(TACN^{Bn3})_2(O_2)]^{2+}$ [7] were used to represent side-on peroxo and bis-μ-oxo species, respectively. The results of these simulations are shown in Figure 6. They indicate that a species containing ca. 40% bis-μ-oxo core should begin to show a clear feature at higher pre-edge energy in the second derivative. Thus, since there is no pre-edge feature at ∼8981 eV in the Cu K-edge spectrum of $[\{Cu(MePY2)\}_2O_2]^{2+}$, it is estimated from the curvature of the observed and calculated derivatives that the mixture could contain at most 40% bis-μ-oxo component, which is consistent with both the resonance Raman and the EXAFS results.

(30) DuBois, J. L.; Mukherjee, P.; Collier, A. M.; Mayer, J. M.; Solomon, E. I.; Hedman, B.; Stack, T. D. P.; Hodgson, K. O. *J. Am. Chem. Soc.* **1997**, *119*, 8578−8579.

Table 1. Summary of EXAFS Curve-Fitting Results for [{Cu(MePY2)}$_2$O$_2$](BArF)$_2$

% Cu−Cu at 2.8 Å (X)	0	20	40	60	80	100
% Cu−Cu at 3.6 Å (Y)	100	80	60	40	20	0
ΔE_0 (eV)	−9.127	−8.637	−9.258	−9.907	−10.584	−11.10
4 Cu−N/O (Å)	1.95	1.95	1.94	1.94	1.94	1.94
σ^2(Å^2)	(0.0086)	(0.0085)	(0.0085)	(0.0086)	(0.0086)	(0.0086)
1 Cu−N (Å)	2.30	2.30	2.31	2.31	2.31	2.31
σ^2(Å^2)	(0.0041)	(0.0053)	(0.0048)	(0.0045)	(0.0042)	(0.0039)
5 Cu−N−C[a] (119°)	2.91	2.96	2.97	2.98	2.99	3.01
σ^2(Å^2)	(0.0082)	(0.0056)	(0.0048)	(0.0046)	(0.0047)	(0.0028)
	3.11	3.16	3.17	3.19	3.19	3.21
	(0.0082)	(0.0056)	(0.0048)	(0.0046)	(0.0048)	(0.0028)
1X Cu−Cu (Å)		2.83	2.84	2.84	2.85	2.85
(σ^2(Å^2))		(0.001)	(0.0021)	(0.0035)	(0.0048)	(0.0044)
1Y (Cu−O−Cu[a] (134°))	3.58	3.57	3.58	3.57	3.57	
(σ^2(Å^2))	(0.0072)	(0.0067)	(0.0054)	(0.0036)	(0.0007)	
	3.76	3.76	3.76	3.76	3.75	
	(0.0090)	(0.0084)	(0.0067)	(0.0045)	(0.0009)	
2 Cu−C−C[a] (167°)	4.37	4.37	4.37	4.36	4.35	4.35
σ^2(Å^2)	(0.0073)	(0.0070)	(0.0071)	(0.0073)	(0.0077)	(0.0069)
	4.41	4.41	4.41	4.40	4.39	4.38
	(0.0074)	(0.0070)	(0.0072)	(0.0074)	(0.0078)	(0.0070)
F[b]	0.100	0.0685	0.0719	0.0752	0.0794	0.110

[a] These components represent a single scattering path (top) and the corresponding multiple scattering path (bottom). For all three body paths, angles were held at a fixed value, indicated in parentheses. [b] Error is given by $\sum[(\chi_{obsd} - \chi_{calcd})^2 k^6]/n]$, where n is the number of data points.

Discussion

The absorption spectrum of [{Cu(MePY2)}$_2$O$_2$]$^{2+}$ in dichloromethane has two bands at 355 and 530 nm, characteristic of a planar side-on peroxide core, as well as an additional band at 410 nm.[17,18] A study of a related series of complexes, where the Cu(PY2) units are linked by an alkyl chain of varying length, established that the absorption band present at 420−490 nm (depending on the length of the linker) was due to a "butterfly" Cu$_2$(O$_2$) core.[10] However, resonance Raman spectra of both solution and solid [{Cu(MePY2)}$_2$O$_2$]$^{2+}$ show the presence of a small amount of bis-μ-oxo isomer; a profile of the symmetric Cu−O core stretch of the [Cu(III)$_2$(O$_2$)]$^{2+}$ core indicates that the absorption band at 410 nm is an μ-O^{2-} → Cu(III) CT band. Hence, qualitatively similar absorption spectra can be obtained for related complexes for two very different reasons; the distortion of the Cu$_2$(O$_2$) core away from planarity allows intensity into a previously forbidden band (at 420−490 nm), and a small amount of the bis-μ-oxo isomer gives an μ-O^{2-} → Cu(III) CT band at 410 nm. Therefore, caution must be exercised when using absorption bands as a fingerprint for the structure of binuclear copper−oxygen complexes.

The crystal structure obtained for [{Cu(MePY2)}$_2$O$_2$]$^{2+}$ gave a copper−copper distance of 3.45 Å and an oxygen−oxygen separation of 1.67 Å, the R value was ∼10% and the displacement parameters were well-behaved.[19,20] This "intermediate" structure is an intriguing possibility if the barrier to interconversion of side-on peroxide and bis-μ-oxo cores is indeed as low as indicated by DFT calculations.[31,32] However the results obtained from EXAFS show that an intermediate Cu−Cu distance of 3.45 Å gives a poor fit to the data, and a significantly better fit is achieved with a mixture of side-on peroxide core (Cu−Cu = 3.6 Å) and a small amount of bis-μ-oxo core (Cu−Cu 2.8 Å). Analysis of the edge region indicates that there is less than 40% bis-μ-oxo present in the solid sample. Resonance Raman spectra obtained for the solid confirm the presence of the bis-μ-oxo and side-on peroxide isomers, the bis-μ-oxo isomer comprising 5−20% of the mixture. Interestingly the weighted average of the Cu−Cu and O−O separations obtained for a mixture of 80% side-on peroxide and 20% bis-μ-oxo are 3.4 and 1.6 Å, respectively. Therefore it appears that the crystal structure represents a mixture of sites in the crystalline solid. There is some precedence for this type of observation: the proposed "bond stretch isomerism" observed in *cis*-mer-MoOCl$_2$(PMe$_2$Ph)$_3$ was due to the presence of mer-MoCl$_3$(PMe$_2$Ph)$_3$;[33] a complex, initially formulated as *trans*-Re(OH)Cl$_3$(PEt$_3$-Ph)$_2$ on the basis of a preliminary X-ray structure determination[34] was found to be a solid solution of *trans*-ReCl$_4$(PEt$_2$Ph)$_2$ in *trans*-Re(O)Cl$_3$(PEt$_2$Ph)$_2$,[35] and Tolman has reported finding a range of Cu−Cu and O−O distances in crystal structures of [Cu$_2$(TACN$^{i\text{Pr}3}$)$_2$O$_2$]$^{2+}$ which was attributed to a mixture of two species, one a side-on peroxide-bridged binuclear copper core.[36] It appears, as stated by Parkin,[33] "the observation of low R values, low esd's and well-behaved thermal parameters are not always sufficient indications of a *true* structure". The intermediate structure obtained from the crystal structure determination of [{Cu(MePY2)}$_2$O$_2$]$^{2+}$ also does not appear to be representative of the true composition.

Side-on Peroxide and Bis-μ-oxo Equilibrium. The factors that govern the presence of bis-μ-oxo and/or side-on peroxide isomers in solution have remained undefined. It has been proposed[36] that the bulky substituents in [Cu$_2$(TACN$^{i\text{Pr}3}$)$_2$O$_2$]$^{2+}$ provide sufficient steric hindrance that the two copper centers are prevented from attaining the 2.8 Å separation associated with a bis-μ-oxo core, and hence the more extended side-on peroxide isomer (Cu−Cu separation of 3.6 Å) is observed. The separation of the two copper atoms certainly seems to play a role. For example, the ligand system [(*m*-XYL-^{i}Pr4)Cu$_2$(CH$_3$-CN)$_2$]$^{2+}$ where a xylyl unit links the isopropyl-substituted TACN ligand is a class B ligand (using the grouping system of Tolman[36]). Therefore, upon oxygenation, the bis-μ-oxo species should be favored under all conditions. However, *intramolecular* oxygenation (where oxygen bridges two copper atoms of the same molecule) yields a side-on peroxide product, and it was

(31) Cramer, C. J.; Smith, B. A.; Tolman, W. B. *J. Am. Chem. Soc.* **1996**, *118*, 11283−11287.
(32) Bercés, A. *Inorg. Chem.* **1997**, *36*, 4831−4837.
(33) Yoon, K.; Parkin, G.; Rheingold, A. L. *J. Am. Chem. Soc.* **1992**, *114*, 2210−2218.
(34) Chatt, J.; Rowe, G. A. *J. Chem. Soc.* **1962**, 4019−4033.
(35) Chatt, J.; Garforth, J. D.; Johnson, N. P.; Rowe, G. A. *J. Chem. Soc. A* **1964**, 601−606.
(36) Tolman, W. B. *Acc. Chem. Res.* **1997**, *30*, 227−237.

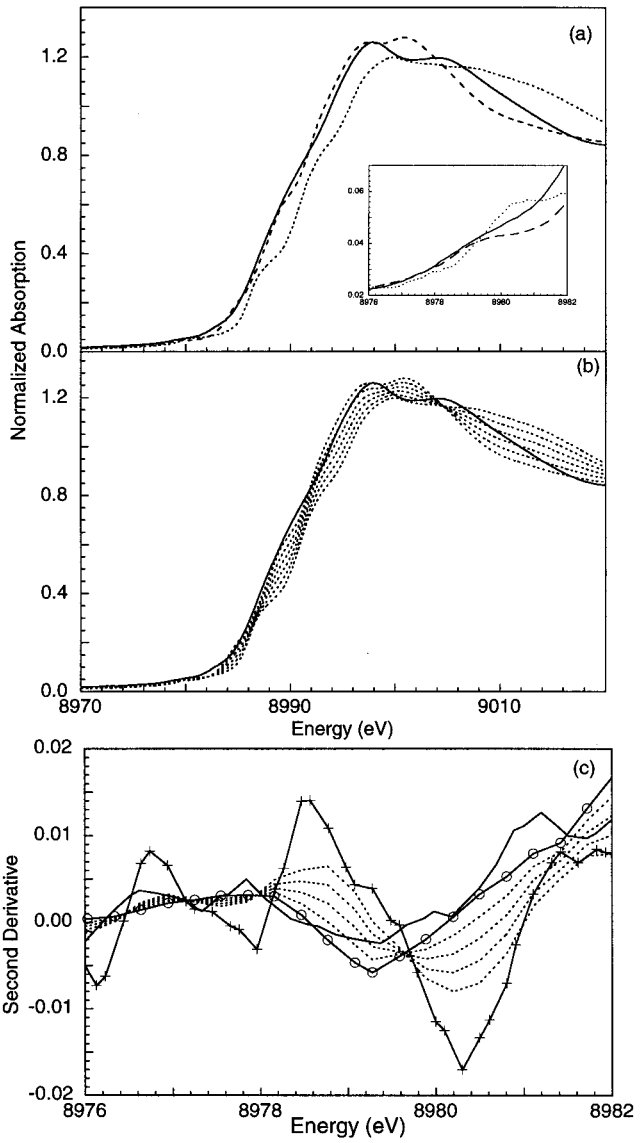

Figure 6. (a) Comparison of the normalized Cu K-edge XAS spectra of $[\{Cu(MePY2)\}_2O_2]^{2+}$ (—), $[Cu(HB(3,5\text{-}Ph_2pz)_3]_2(O_2)$ (- - -) and $[Cu_2(TACN^{Bn3})_2O_2]^{2+}$ (•••). The inset amplifies the pre-edge region. (b) Calculated edges using varying proportions of $[Cu(HB(3,5\text{-}Ph_2pz)_3]_2(O_2)$ and $[Cu_2(TACN^{Bn3})_2O_2]^{2+}$ (•••), and the spectrum of $[\{Cu(MePY2)\}_2O_2]^{2+}$ (—). The simulated spectra represent the following ratios of side-on to bis-μ-oxo character: 80:20, 60:40, 40:60, and 20:80. (c) The second derivative of the data shown in (b), over the pre-edge region. For clarity the models are shown as, $[Cu(HB(3,5\text{-}Ph_2pz)_3]_2(O_2)$ (○) and $[Cu_2(TACN^{Bn3})_2O_2]^{2+}$ (+).

proposed that the stiff arene ring-containing linker holds the Cu atoms sufficiently far apart so as to favor the side-on peroxide core.[37]

Further, data obtained from spectroscopically and structurally characterized Cu_2O_2 intermediates suggest that amine-based ligands such as those of Tolman and Stack favor the bis-μ-oxo complex, whereas the pyridine-based ligands of Karlin favor the side-on peroxide core. The more basic, σ-donating amine ligands may be more suitable than pyridine to enhance back-donation into the σ^* orbital of the side-on peroxide and cleave the O−O bond to form the bis-μ-oxo core. For example, in a recent study of $[Cu_2(NO_2\text{-}XYL)(O_2)]^{2+}$ (pyridine ligation) it was

Scheme 2

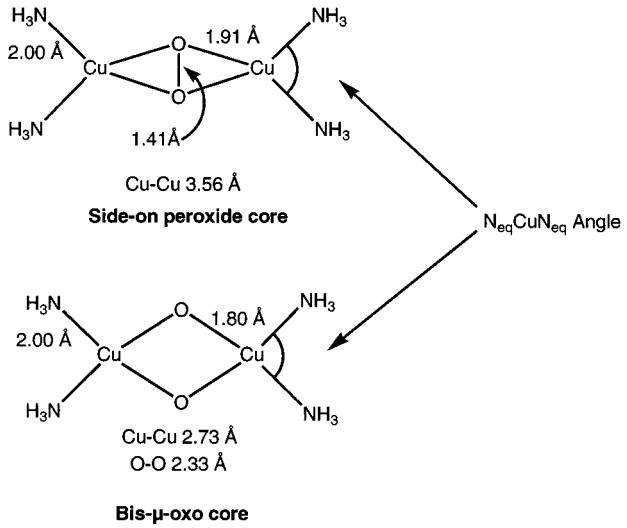

established using resonance Raman spectroscopy that the product from *intermolecular* oxygenation (where oxygen bridges two copper atoms of different molecules) was a side-on peroxide core.[16] Conversely, *intermolecular* oxygenation of $[(m\text{-}XYL\text{-}^{i}Pr4)Cu_2O_2]^{2+}$ (amine nitrogen ligation) yielded the bis-μ-oxo core exclusively.[37]

Also the number of nitrogen donors is doubtless an important factor which affects the equilibrium between side-on peroxide and bis-μ-oxo cores as indicated by the results of Alvarez and co-workers.[38] From the work of Mahadevan et al.,[8] the two amino-nitrogen donors of the peralkylated cyclohexanediamine ligands have been shown to be sufficient to stabilize the bis-μ-oxo core. Interestingly, no direct evidence has been obtained for the existence of a side-on peroxide core with only two nitrogen donors per copper.[39]

The identification of the presence of some bis-μ-oxo isomer for both solid and solution $[\{Cu(MePY2)\}_2O_2]^{2+}$ but not for the closely related $[Cu_2(N\textit{n}PY2)(O_2)]^{2+}$ complexes is interesting since the ligand systems MePY2 and N*n*PY2 differ only in the alkyl-chain linker which should not change the steric hindrance, the number of nitrogen donors or the chemical nature of the ligands.

Another factor may be the geometry of the nitrogen ligation around the copper centers. The $N_{eq}CuN_{eq}$ bite angle of the Cu_2O_2 cores, defined by two equatorial nitrogen donors bound to a copper atom, is found to be 89° in crystal structures of the bis-μ-oxo cores.[7,8] The same angle in the side-on peroxide-bridged dicopper $[Cu(HB(3,5\text{-}i\text{-}Pr_2pz)_3)]_2(O_2)$[13] is 93° and in oxyhemocyanin it is found to be 94−99°.[3] Thus, the bis-μ-oxo cores are characterized by a smaller $N_{eq}CuN_{eq}$ angle than the side-on peroxide cores consistent with the large O−Cu−O angle of the bis-μ-oxo core. Density functional calculations using the ADF program have been performed upon planar, $[(NH_3)_4Cu_2(\mu\text{-}O)_2]^{2+}$, and $[(NH_3)_4Cu_2(\mu\text{-}\eta^2\text{:}\eta^2)(O_2)]^{2+}$ cores with $N_{eq}CuN_{eq}$ angles of 97, 93, 89, and 86°, maintaining D_{2h} symmetry (Scheme 2; coordinates included in Supporting Information).

(37) Mahapatra, S.; Kaderli, S.; Llobet, A.; Neuhold, Y.-M.; Palanché, T.; Halfen, J. A.; Young, V. G.; Kaden, T. A.; Que, L., Jr.; Zuberbühler, A. D.; Tolman, W. B. *Inorg. Chem.* **1997**, *36*, 6343−6356.

(38) Liu, X.-Y.; Palacios, A. A.; Novoa, J. J.; Alvarez, S. *Inorg. Chem.* **1998**, *37*, 1202−1212.

(39) (a) Ryan, S.; Adams, H.; Fenton, D. E.; Becker, M.; Schindler, S. *Inorg. Chem.* **1998**, *37*, 2134−2140. (b) Casella, L.; Monzani, E.,; Gulloti, M.; Cavagnino, D.; Cerina, G.; Santagostini, L.; Ugo, R. *Inorg. Chem.* **1996**, *35*, 7516−7525. (c) Casella, L.; Gullotti, M.; Pallanza, G.; Rigoni, L. *J. Am. Chem. Soc.* **1988**, *110*, 4221−4227. (d) Gelling, O. J.; van Bolhuis, F.; Meetsma, A.; Feringa, B. L. *J. Chem. Soc., Chem. Commun.* **1988**, 552−554. (e) Menif, M.; Martell, A. E.; Squattrito, P. J. Clearfield, A. *Inorg. Chem.* **1990**, *29*, 4723−4729.

Table 2. Total Bonding Energies (eV) of $[(NH_3)_4Cu_2(\mu\text{-}O)_2]^{2+}$ and $[(NH_3)_4Cu_2(\mu\text{-}\eta^2\text{:}\eta^2)(O_2)]^{2+}$ with Varying $N_{eq}CuN_{eq}$ Angle

$N_{eq}CuN_{eq}$ angle (deg)	total bonding energy (eV)	
	$[(NH_3)_4Cu_2(\mu\text{-}O)_2]^{2+}$	$[(NH_3)_4Cu_2(\mu\text{-}\eta^2\text{:}\eta^2)(O_2)]^{2+}$
97	−85.32	−77.06
93	−85.28	−76.98
89	−85.20	−76.87
86	−85.09	−76.73
	$\Delta = 0.23$ eV	$\Delta = 0.33$ eV

The total bonding energies (eV) calculated for the cores are given in Table 2. From these energies, the bis-μ-oxo core is found to be closer to the structure corresponding to the energy minimum of a planar $[(NH_3)_4Cu_2(O)_2]^{2+}$ core. However, it can be seen that the increase in total bonding energy of the side-on peroxide core upon compression of the $N_{eq}CuN_{eq}$ angle from 97 to 86° (0.33 eV) is larger than that for the bis-μ-oxo core (0.23 eV), i.e., the side-on peroxide core is perturbed to a greater extent when the $N_{eq}CuN_{eq}$ angle is more acute. In the side-on peroxide core the Cu $d_{x^2-y^2}$ orbital, which is in the N_2CuO_2 plane and has lobes that point at the ligands, is partially occupied, and compressing the $N_{eq}CuN_{eq}$ angle destabilizes the $d_{x^2-y^2}$-containing molecular orbitals. The HOMO of the side-on peroxide core, which has substantial Cu $d_{x^2-y^2}$ character is destabilized by 0.14 eV upon changing the $N_{eq}CuN_{eq}$ angle from 93 to 86°. However, in the bis-μ-oxo core, the $d_{x^2-y^2}$ orbital is unoccupied (i.e., square planar Cu(III)), and hence, changing the geometry of the equatorial nitrogen atoms effects the overall bonding energy to a much lesser degree. Therefore, a tridentate nitrogen donor ligand with a small bite angle, for example, TACN, where only two carbon atoms separate the N-donor atoms, will favor the bis-μ-oxo isomer. Alternatively, the combination of a pyridine-based ligand and a larger bite angle (three carbon atoms of the ligand backbone separate the N-donors in N*n*PY2) should favor the side-on peroxide isomer. Experimental data appear consistent with this trend. For a solution of $[Cu_2(TACN^{iPr3})_2(\mu\text{-}O)_2]^{2+}$ the sterically demanding isopropyl groups force a larger (than 89°) $N_{eq}CuN_{eq}$ angle, and the side-on peroxide is the dominant species present.[9] The bis-μ-oxo isomer is observed exclusively in a solution of $[Cu_2(TACN^{iPr2Bn})_2(\mu\text{-}O)_2]^{2+}$; thus, replacing one isopropyl group with CH_2-Ph, which is less bulky at the α-carbon, changes the species that dominates. It is interesting to note that the crystal structure obtained for the bis-hydroxy-containing decomposition product of $[Cu_2(TACN^{iPr2Bn})_2(\mu\text{-}O)_2]^{2+}$ shows the CH_2-Ph substituent located *in the equatorial plane*.[7] Hence, the less sterically demanding CH_2-Ph group allows the smaller N_{eq}-CuN_{eq} angle, and the bis-μ-oxo isomer is observed.

For the N*n* series, EXAFS data[40] for $[Cu_2(NnPY2)O_2]^{2+}$, where $n = 3$ and 4 indicate that the axial ligand at each copper center is pyridine, and therefore the amino-nitrogen, via which the two copper centers are linked, is in the equatorial plane. It has been established, using resonance Raman spectroscopy, that the oxygen-bound intermediate is a side-on bridged peroxide moiety; no evidence for the presence of the bis-μ-oxo isomer has been observed.[10] Conversely, for $[\{Cu(MePY2)\}_2O_2]^{2+}$, the alkyl-chain linker has been replaced with a methyl group and a small percentage (<20%) of the bis-μ-oxo isomer is observed in solid and solution. The appearance of a small amount of the bis-μ-oxo isomer may indicate the equatorial nitrogen ligation of $[\{Cu(MePY2)\}_2O_2]^{2+}$ is unconstrained and the small N_{eq}-CuN_{eq} bite angle characteristic of the bis-μ-oxo isomer is possible, though not strongly favored. The observation of the side-on peroxide isomer exclusively in solutions of $[Cu_2(NnPY2)(O_2)]^{2+}$ suggests that the alkyl-chain linker affects the equatorial N ligation and could increase the effective bite angle of the N-donor ligand. Combined with the pyridine-based ligation, only the side-on peroxide isomer is observed.

Scheme 3

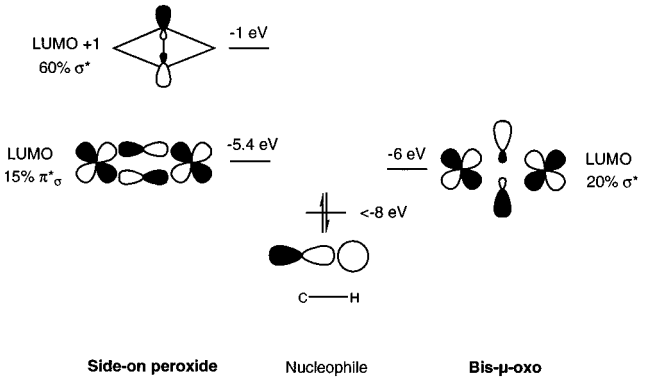

Hydrogen-Atom Abstraction. It has been found that solutions of $[\{Cu(MePY2)\}_2O_2]^{2+}$ and $[Cu_2(NnPY2)(O_2)]^{2+}$ show different reactivites toward exogenously added hydrocarbon substrates.[18] Solutions of $[\{Cu(MePY2)\}_2O_2]^{2+}$ react with 1,4-cyclohexadiene and dihydroanthracene to give benzene and anthracene, respectively, in yields greater than 70%, and the addition of dimethylaniline gives products from an N-dealkylation reaction.[41] The series of complexes $[Cu_2(NnPY2)(O_2)]^{2+}$ show very little reactivity with exogenous substrates. Therefore, removing the alkyl-chain linker from the amino nitrogen alters the reactivity of the Cu_2O_2 core. These differences in reactivity may be due to several factors, including the increased accessibility of the Cu_2O_2 core in $[\{Cu(MePY2)\}_2O_2]^{2+}$ and the presence of a small amount (<10%) of the bis-μ-oxo isomer in solution $[\{Cu(MePY2)\}_2O_2]^{2+}$. Indeed, it has been shown that the $[Cu(III)(\mu\text{-}O)_2]^{2+}$ complex performs ligand dealkylation reactions at the site of the weakest C−H bond; the reactions show a deuterium isotope effect, implicating a rate-determining step which involves a C−H cleavage pathway.[8,42]

Frontier molecular orbital theory has been used to assess the relative reactivities of the side-on peroxide and bis-μ-oxo isomers.[16] A small splitting between the HOMO of the nucleophile and the LUMO of the electrophile will yield a large interaction energy for the reaction. Also, the symmetry of the interacting orbitals and the coefficients of these relevant frontier molecular orbitals have to be considered. The LUMO (capable of accepting an electron) of the bis-μ-oxo core at approximately −6 eV comprises 62% copper $d_{x^2-y^2}$ orbitals and 20% O^{2-} σ* (Scheme 3). The dominant lobe of the σ* orbital extends beyond the Cu_2O_2 core and would be expected to have good overlap with the lower lying (<−8 eV), occupied, σ-bonded C−H containing MO of the H atom "donor", in a hydrogen-atom abstraction reaction.

The LUMO of the side-on peroxide core which is found at −5.4 eV, comprises 70% Cu $d_{x^2-y^2}$ and 15% peroxide π^*_σ orbital (O p orbitals parallel to the Cu−Cu axis) would not have a favorable, symmetry-allowed interaction with the occupied σ-bonded C−H-containing molecular orbital of the H-atom donor. The LUMO+1 of the side-on peroxide core is similar to the LUMO of the bis-μ-oxo core; it comprises 60% σ* but

(40) Blackburn, N. J.; Strange, R. W.; Farooq, A.; Haka, M. S.; Karlin, K. D. *J. Am. Chem. Soc.* **1988**, *110*, 4263−4272.

(41) Liang, H.-C.; Karlin, K. D., private communication.

(42) Mahapatra, S.; Halfen, J. A.; Tolman, W. B. *J. Am. Chem. Soc.* **1996**, *118*, 11575−11586.

Scheme 4

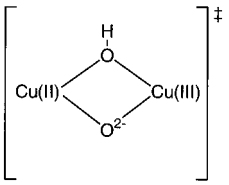

it is found approximately 5 eV *to higher energy* than the LUMO of the bis-μ-oxo core. Despite the sizable percentage of σ^* present in the LUMO+1 of the side-on peroxide core, the large energy gap between the LUMO+1 and the C−H-containing MO of the nucleophile is expected to make H-atom abstraction reactions less favorable for side-on peroxide core than bis-μ-oxo cores. Therefore, for a solution of $[\{Cu(MePY2)\}_2O_2]^{2+}$ where there is a mixture of side-on peroxide and bis-μ-oxo isomers,[18] it would be expected from the application of frontier molecular orbital theory that the bis-μ-oxo isomer is responsible for the H-atom abstraction reactions observed with exogenously added substrate, via a σ^* LUMO mechanism; this reactivity would be reduced for the $[Cu_2(NnPY2)(O_2)]^{2+}$ complexes since there is no detectable amount of bis-μ-oxo isomer present in solution.[10]

A study of hydrocarbon oxidations by oxometal reagents such as MnO_4^-, by Mayer and co-workers,[43] has shown that the enthalpy of reaction and hence the rate of H-atom abstraction (as H$^\bullet$) by these reagents is correlated to the difference between C−H bond strength of the donor and O−H bond strength of the product. The bond dissociation energy of the O−H bond in the product can be calculated using the pK_a of the O−H bond and the $E°$ of the unprotonated complex. The abstraction of H$^\bullet$ by side-on peroxide and bis-μ-oxo cores will give the same initial "intermediate" (Scheme 4).

The pK_a of the O−H group will be the same for the two isomers, and hence any difference in the relative rates of reaction will be expressed by $E°$. Reduction potentials are not available for both isomers, but the energy of the LUMO of both cores offers an approximation to $E°$. As stated earlier, the LUMO energies of the side-on peroxide and bis-μ-oxo cores are separated by 0.6 eV, the LUMO of the bis-μ-oxo core to deeper binding energy. Calculations, using multiconfigurational ab initio theory performed by Cramer and co-workers[44] upon the bis-μ-oxo and side-on peroxide cores found the LUMO of the side-on peroxide core to be ~1.1 eV to deeper energy than the LUMO of the bis-μ-oxo core. A deeper energy LUMO indicates a greater affinity for electrons and therefore, a higher value of $E°$. Thus, without taking into account the *nature* of the LUMO (i.e., its symmetry-allowed interactions with the relevant MO of the nucleophile) it would be predicted, from thermodynamic arguments, that the reactivity of the side-on peroxide core with respect to H-atom abstraction would be higher than that of the bis-μ-oxo core, or at least that their reactivities would be similar. However, it is observed[37,42] that side-on peroxide-containing binuclear copper complexes are less reactive than bis-μ-oxo cores with respect to H-atom abstraction reactions.

Importantly, it should be noted in the discussion of the relative reactivities of the side-on peroxide and bis-μ-oxo cores that there is a large Franck−Condon barrier to the reductive cleavage of the peroxide O−O bond, particularly by one electron.[45] However, in the bis-μ-oxo core, the O−O is already reductively cleaved by two electrons, giving two Cu(III) centers. The driving force for a hydrogen-atom abstraction reaction by the bis-μ-oxo core is therefore the Cu(III)/Cu(II) redox couple and is highly favorable.

Summary

In summary it has been established through the use of X-ray absorption spectroscopy and resonance Raman spectroscopy that the intermediate geometry given by the crystal structure is not representative of the true structure. Rather the crystalline material is an example of a solid solution comprising approximately 20% of the bis-μ-oxo core and 80% of the side-on peroxide isomer. A number of factors which may affect the ratio of bis-μ-oxo and side-on peroxide cores obtained in equilibrium, including the equatorial N−Cu−N bite angle, have been detailed. Finally, the relative reactivites of the two isomers with respect to H-atom abstraction via a σ^* mechanism have been addressed using frontier molecular orbital theory and thermodynamic and kinetic barrier arguments.

Acknowledgment. This work was supported by grants from the National Institutes of Health (DK31450 (E.I.S.), GM28962 (K.D.K.), and RR01209 (K.O.H.)) and by the National Science Foundation (CHE9423181 (K.O.H.). SSRL operations are funded by the Department of Energy, Office of Basic Energy Sciences. The Biotechnology Program is supported by the National Institutes of Health, National Center for Research Resources, Biomedical Technology Program and by the Department of Energy, Office of Biological and Environmental Research. The authors would like to thank Victor Young, Jr., University of Minnesota, for the crystal structure determination and Kent Nakagawa and Jennifer DuBois for providing data on the $([Cu(HB(3,5\text{-}Ph_2pz)_3]_2(O_2)$ and $[Cu_2(TACN^{Bn3})_2O_2]^{2+}$ model complexes, respectively.

Supporting Information Available: Tables of angles for side-on peroxide core and bis-μ-oxo core (PDF). This material is available free of charge via the Internet at http://pubs.acs.org.

JA983444S

(43) Gardner, K. A.; Mayer, J. M. *Science* **1995**, *269*, 1849−1851.
(44) Cramer, C. J.; Smith, B. A.; Tolman, W. B. *J. Am. Chem. Soc.* **1996**, *118*, 11283−11287.
(45) Shin, W.; Sundaram, U. M.; Cole, J. L.; Zhang, H. H.; Hedman, B.; Hodgson, K. O.; Solomon, E. I. *J. Am. Chem. Soc.* **1996**, *118*, 3202−3215.